© 1984 Geologie en Mijnbouw 0016-7746/84/6302-0213 $ 2.50/0

THE EFFECT OF CARBON DIOXIDE ON PHASE RELATIONSHIPS FOR SYNTHETIC LHERZOLITE AND HARZBURGITE[1]

PETER J. WYLLIE[2]

ABSTRACT

Wyllie, P. J. 1984 The effect of carbon dioxide on phase relationships for synthetic lherzolite and harzburgite. In: H. J. Zwart, P. Hartman & A. C. Tobi (eds): Ophiolites and ultramafic rocks – a tribute to Emile den Tex – Geol. Mijnbouw 63:213-219.

The system CaO-MgO-SiO_2 -CO_2 includes mineral assemblages corresponding to model lherzolite: forsterite(Fo) + orthopyroxene(Opx) + clinopyroxene(Cpx), and model harzburgite: Fo + Opx, as well as model websterite and wehrlite. When fully carbonated, the peridotites are converted to limestones: dolomite(Do) + magnesite(Mc) + quartz(Qz), or Mc + Qz. When partly carbonated, the peridotites are converted to carbonate-lherzolite and magnesite-harzburgite, which cannot coexist with CO_2. Available experimental and calculated reaction data are presented for carbonate-lherzolite: (6) Opx + Do = Cpx + Fo + CO_2 and (6A) Opx + Cc = Cpx + Fo + CO_2, where Do is dolomite and its solid solution, and Cc is magnesium calcite; for magnesite-harzburgite: (3) MC + En = Fo + CO_2; for websterite + carbonate: (0) Mc + Cpx = Do + Opx and (01) Do + Cpx = Cc + Opx; and for carbonate-wehrlite: (9)Do + Cpx = Fo + Cc + CO_2. Conditions for the occurrence of dolomite(stoichiometric)-lherzolite are evaluated. Comparison of fossil geotherms deduced from kimberlite nodules with the phase diagrams for model harzburgite and lherzolite, and solidus curves with H_2O present, indicates that partially melted lherzolite may coexist with solid magnesite-harzburgite between about 175 and 195 km depth. Dissociation of magnesite could disrupt the harzburgite nodules during eruption, distributing low-calcium garnet through kimberlite.

INTRODUCTION

Ultramafic rocks, composed of olivines and pyroxenes, are not abundant in the crust, but their origin has occupied many pages in the literature. With plate tectonics, their distribution has taken on special significance as scars marking the remnants of vanished ocean basins, and their structures have assumed importance as guides to the dynamics of mantle flow.

The upper mantle is a great reservoir of peridotites. Peridotites may be transported from this reservoir into the crust, or they may be generated within the crust by two means. Crystallization differentiation of basic magma yields precipitates of ultrabasic rocks. The metamorphism or metasomatism of siliceous dolomites yields assemblages including the minerals of peridotites; the reactions relating dolomites and peridotites have been reviewed by BOWEN (1940) and WYLLIE & HUANG (1976a).

In this contribution, I review recent experimental and theoretical data (mainly at high pressures) which demonstrate the effect of CO_2 on the mineralogy of peridotite, and the reactions which can yield peridotite from siliceous dolomite of suitable composition. The effect of H_2O and the involvement of serpentine is omitted from this brief presentation, but the effect of H_2O on melting reactions in the mantle is introduced.

SYNTHETIC 'MODEL' PERIDOTITES

The composition of the mantle and variations in peridotite mineralogy as a function of depth can be well represented in the system MgO-FeO-CaO-Al_2O_3-Na_2O-SiO_2 (e.g. RINGWOOD, 1966) and the simplified system CaO-MgO-Al_2O-SiO_2 has been used successfully as a system for modelling the mineralogy of peridotite (e.g. O'HARA, 1967; MACGREGOR, 1967). BOWEN (1940) used the system CaO-MgO-SiO_2-CO_2 for representation of the minerals in siliceous dolomites, and this is also adequate for modelling the major minerals of many peridotites; with omission of Al_2O_3, the accessory aluminous

---

[1] Manuscript received: 1983-09-30.
Manuscript accepted: 1984-05-01.

[2] Division of Geological and Planetary Sciences, California Institute of Technology, Pasadena, Cal. 91125, U.S.A.

minerals plagioclase, spinel and garnet are absent. The minerals of peridotites occurring in this system include forsterite (Fo), enstatite (En), orthopyroxene (Opx), diopside (Di), and clinopyroxene (Cpx); the minerals of limestones include calcite and its solid solution (CC, Cc), dolomite and its solid solution (Do), Magnesite and its solid solution (MC, Mc), and quartz and other polymorphs of SiO_2 (Qz).

There are three ways to approach the phase relationships in the system $CaO\text{-}MgO\text{-}SiO_2\text{-}CO_2$. The first is to consider all of the minerals present in the system, and to determine all possible reactions that can occur among them, with their variations as a function of pressure and temperature. This approach reveals a large number of possible reactions, but the present state of experiments and thermochemical data is such that it is commonly impossible to choose among various options (see SKIPPEN, 1971, 1974). The second approach is to consider specific reactions which involve minerals of particular interest for a petrological problem. These reactions encompass a range of bulk compositions and introduce mineral assemblages which may have little relationship to the problem of interest. A third approach is to define a bulk composition and to determine the mineral assemblage it forms at various temperatures and pressures.

The available experimental and theoretical data for many reactions in the system $CaO\text{-}MgO\text{-}SiO_2\text{-}CO_2$ were recently reviewed and combined with new experimental data by WYLLIE ET AL. (in press) for compilation of a revised array of reactions. In this contribution, we will deal with particular reactions, and concentrate on the phase assemblages produced which correspond to peridotite bulk compositions. Peridotite mineral assemblages occurring in the system include model lherzolite (Fo + Opx + Cpx) and harzburgite (Fo + Opx, Fo + En). These assemblages may be carbonated by CO_2 at high pressures or low temperatures, and when fully carbonated they are transformed into limestones in which CO_2 can coexist with Do + Mc + Qz, and MC + Qz, respectively. When partly carbonated, the model lherzolite and harzburgite are converted to dolomite-lherzolite (Do + Fo + Opx + Cpx) and magnesite-harzburgite (MC + Fo + En), respectively, which cannot coexist with CO_2. Other model peridotites are wehrlite (Fo + Cpx) and websterite (Opx + Cpx).

Following the numbering system adopted by WYLLIE & HUANG (1975, 1976b) and WYLLIE ET AL. (in press), the reactions of particular interest are:
for model lherzolite,

$$\text{Opx} + \text{Do} = \text{Cpx} + \text{Fo} + CO_2 \tag{6}$$

for model harzburgite,

$$\text{MC} + \text{En} = \text{Fo} + CO_2 \tag{3}$$

for model websterite,

$$\text{Mc} + \text{Cpx} = \text{Do} + \text{Opx} \tag{0}$$

and

$$\text{Do} + \text{Cpx} = \text{Cc} + \text{Opx} \tag{01}$$

and for model wehrlite,

$$\text{Do} + \text{Cpx} = \text{Fo} + \text{Cc} + CO_2 \tag{9}$$

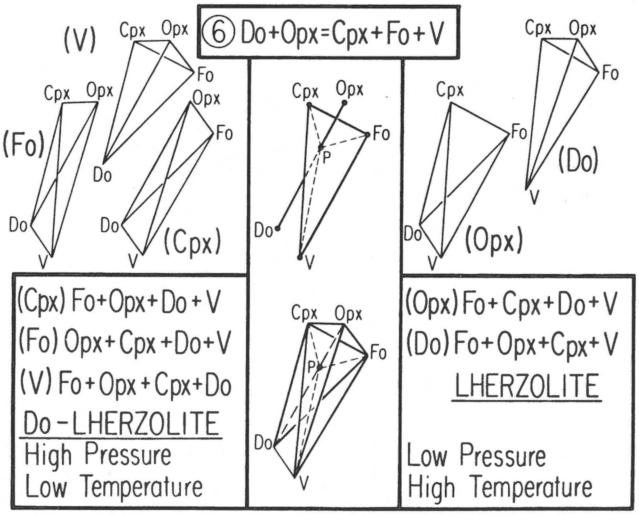

Fig. 1.
Geometry of the tie-figure for reaction (6) from within the tetrahedron $CaO\text{-}MgO\text{-}SiO_2\text{-}CO_2$, with the groups of four-phase tetrahedra which comprise the five-phase tie-figure on either side of the reaction. Abbreviations, see text.

CARBONATION OF MODEL LHERZOLITE, REACTION (6)

Fig. 1 illustrates the complete tie-figure for the reaction, and the phase assemblages occurring on either side of the reaction curve. The assemblages of interest are lherzolite with CO_2, and the partly carbonated dolomite-lherzolite without CO_2. Notice that for other bulk compositions, phase assemblages with CO_2 correspond to partly carbonated dolomite-harzburgite, dolomite-websterite, and dolomite-wehrlite.

All published invariant curves for the reaction are shown in Fig. 2, with a simplified projection of the reaction tie-figure illustrated in the inset (with lines to CO_2 omitted for clarity). There are no experimental data below 15 kbar. WYLLIE ET AL. (in press) gave reasons for selecting as the best curve the one passing through the reserved run brackets, and extrapolated down to low pressures along the EKH curve calculated by EGGLER ET AL (1976).

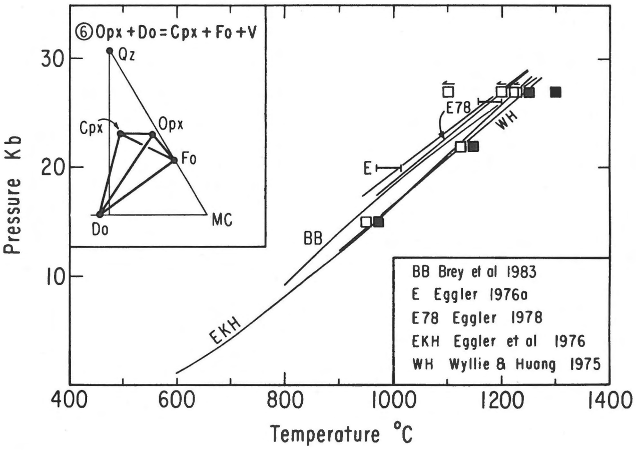

Fig. 2.
Comparison of experimental and theoretical results for reaction (6) in $CaO\text{-}MgO\text{-}SiO_2\text{-}CO_2$, as reviewed by Wyllie at al. (in press).

Fig. 2 indicates that mineral compositions in the lherzolite assemblage are forsterite, pyroxenes, coexisting across the solvus, and a calcic dolomite. WYLLIE ET AL. (in press) determined the compositions of some carbonates and pyroxenes in this reaction with electron microprobe and x-ray diffraction, with results at 27 kbar shown in Fig. 3. The reaction is defined by the mineralogical bracket of runs 1068 and 1067, but the situation is complicated by formation of a trace of liquid in run 1068, which is certainly responsible for the wide spread and change in composition of the carbonate compared with that in runs 1058 and 1073. At temperatures below 1100°C at 27 kbar, the dolomite in the subsolidus assemblage Opx + Cpx + Do + V is slightly calcic, but it changes to magnesian calcite (Cc) with 22% $MgCO_3$ at 1220°C. The composition of carbonate is also highly calcic at lower pressures. At 15 kbar, where the reaction temperature is below the crest of the calcite-dolomite solvus (compare Fig. with solvus in Fig. 3), the carbonate composition is on the $CaCO_3$ side of the solvus, and it must be termed magnesian calcite (Cc). It has been customary to define the invariant reaction (6) at mantle pressures, as illustrated in Fig. 1 and 2, terms of a dolomite solid solution (WYLLIE & HUANG, 1976b; EGGLER, 1978). However, the composition of the carbonate solid solution is such that at pressures and temperatures below the calcite-dolomite solvus crest, the reaction must be defined as:

$$\text{Opx} + \text{Cc} = \text{Cpx} + \text{Fo} + CO_2 \qquad (6A)$$

CARBONATION OF MODEL HARZBURGITE, REACTION (3)

The position of this reaction was defined by NEWTON & SHARP (1975), as shown in Fig. 4, and confirmed by the runs of

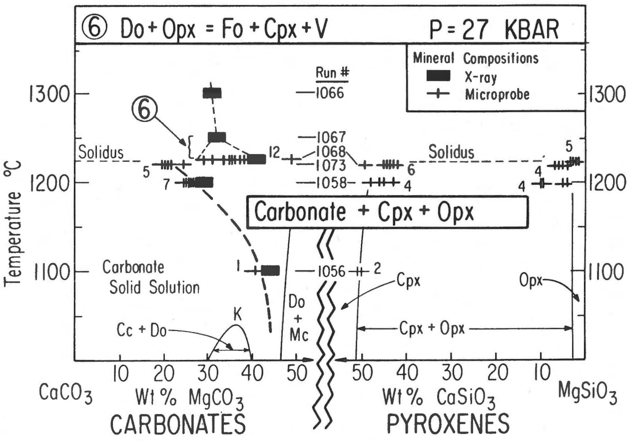

Fig. 3.
Compositions of carbonates and pyroxenes for reaction (6) and at temperatures below reaction (6), at 27 kbar, compared with solvus curves for calcite-dolomite and orthopyroxene-clinopyroxene. Determinations by W.-L. Huang, as reported in Wyllie et al. (in press).

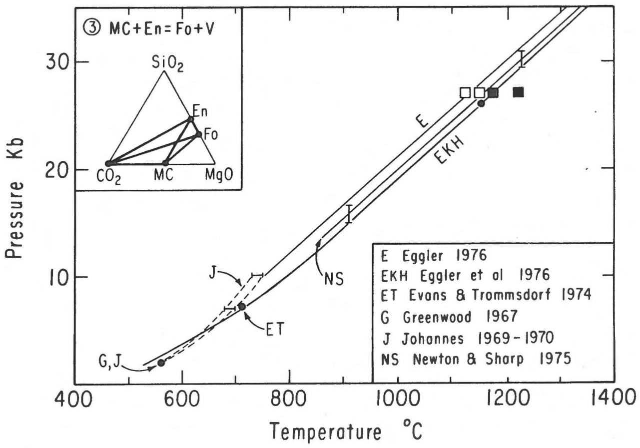

Fig. 4.
Comparison of experimental and theoretical results for reaction (3) in $MgO\text{-}SiO_2\text{-}CO_2$, as reviewed by Wyllie et al. (in press).

WYLLIE ET AL. (in press), who also reviewed the other published curves which are shown for comparison. Reaction (3) is located at somewhat higher pressure and lower temperature than reaction (6). Addition of component CaO to assemblage MC + En + Fo + V produces a divariant assemblage of Mc + Opx + Fo + V, which becomes univariant when the composition of the magnesite solid solution reaches the solvus, introducing dolomite and generating the reaction:

$$\text{Mc} + \text{Opx} = \text{Fo} + \text{Do} + Co_2 \qquad (4)$$

This is the quarternary equivalent of ternary reaction (3), and is situated about 5°C higher than reaction (3) (EGGLER, 1978).

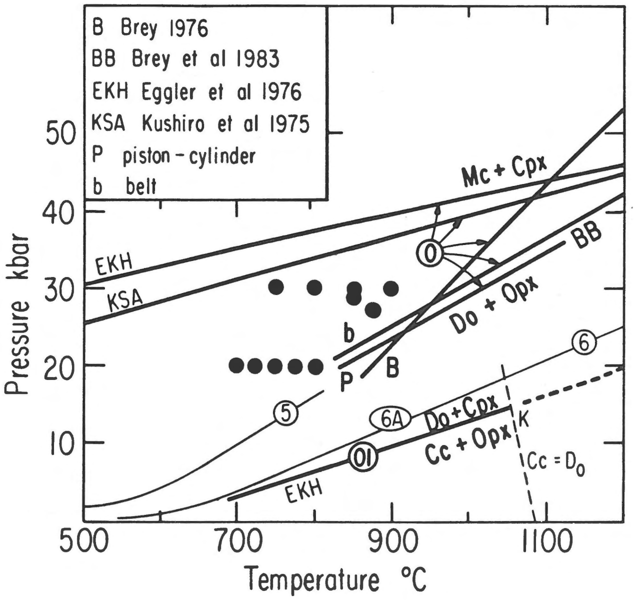

Fig. 5.
Comparison of experimental and theoretical results for degenerate reactions (0) and (01) on the pyroxene-carbonate surface through $CaO-MgO-SiO_2-CO_2$, with closed circle runs by A. P. Byrnes, as reviewed by Wyllie et al. (in press).

WEBSTERITE + CARBONATES

There are two vapor-absent exchange reactions involving pyroxenes and carbonates which have significance for websterites and lherzolite. Reactions (0) and (01) are degenerate, because the carbonate and pyroxene compositions are coplanar. The minerals define a plane through the system $CaO-MgO-SiO_2-CO_2$ which represents a particular degree of carbonation. The degenerate reactions occurring on the plane produce mineral assemblages which may exist alone, or under suitable conditions, with forsterite, or quartz, or vapour.

Experimental and theoretical definition of these solid-solid exchange reactions is difficult, as indicated by the large differences among the five published curves for reaction (0), illustrated in Fig. 5. WYLLIE ET AL. (in press) adopted the curve BB-p as the best available. Fig. 5 shows the position of one calculated curve for reaction (01), but WYLLIE ET AL. (in press) concluded from the geometry of phase relationships that reaction (01) had to be situated at a pressure higher than reaction (6)-(6A). Note that reaction (01) terminates at a critical end-point (K) on the crest of the calcite-dolomite solvus (Cc-Do).

The two reactions (0) and (01) divide the PT field into three areas within which websterite coexists with different carbonates. Calcite solid solution occurs in the low pressure area below reaction (01), dolomite solid solution in the intermediate pressure interval, and magnesite solid solution at the highest pressures above reaction (0).

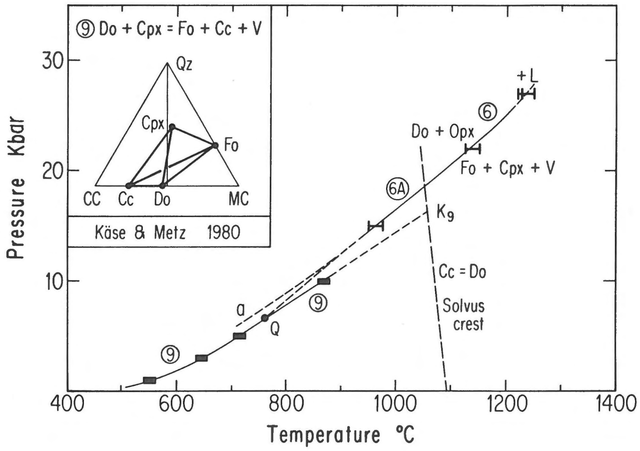

Fig. 6.
Experimental results for reaction (9) in $CaO-MgO-SiO_2-CO_2$, according to Käse & Metz (1980), based on experiments with about 10 mole per cent H_2O to enhance reaction; accuracy ± 10°C. Reaction (6)-(6A) is drawn through the run brackets of Wyllie at al. (1983), transferred from Fig. 2. Linear extrapolation of reaction (6A) intersects reaction (9) at point Q.

CARBONATION OF MODEL WEHRLITE, REACTION (9)

KÄSE & METZ (1980) determined the position of reaction:

$$Do + Cpx = Fo + Cc + CO_2 \qquad (9)$$

to 10 kbar, as shown in Fig. 6. If extrapolated to higher pressures, the curve terminates at K_9, a critical end-point at the crest of the calcite-dolomite solvus, Cc = Do.

The experimentally determined part of reaction (6) is transferred from Fig. 2, and identified in Fig. 6 as reaction (6A) at temperatures below the crest of the calcite-dolomite solvus. Linear extrapolation of this curve to lower pressures produces an intersection with reaction (9) at point Q. No intersection occurs, however, if the extrapolated curve is slightly bent, as shown by the line (6A)-a.

If the reaction curves (6A) and (9) do intersect, this generates an invariant point, Q, for the assemblage:

$$Cc + Do + Cpx + Opx + Fo + CO_2$$

Schreinemaker's rules provide the array of univariant reactions around this point as illustrated in Fig. 7. The arrangement of reactions (9) and (6A) required by the theoretical analysis differs from that indicated by the available experimental data, as shown by the upper left diagram in Fig. 7, and in Fig. 6.

CALCITE - AND DOLOMITE-LHERZOLITE

The reactions (0) and (01) in Fig. 5 divide the degenerate assemblages for carbonate-websterite into magnesite-websterite, dolomite-websterite, and calcite-websterite. Forsterite can coexist with these assemblages at pressures above reaction (01), with the definition of stability fields for magnesite-lherzolite and dolomite-lherzolite. The relationships between dolomite-lherzolite and calcite-lherzolite are, however, more complicated, and part of the complication involves the calcite-dolomite solvus.

At pressures above the solvus crest, model carbonate-lherzolite has been described as dolomite-lherzolite (WYLLIE & HUANG, 1976b; EGGLER, 1978), although the dolomite composition may range widely between dolomite and calcite compositions. WYLLIE & HUANG (1975) referred to calcic dolomite with about 70% $CaCO_3$, and the determination of this composition is illustrated in Fig. 3. At pressures where the curve passes below the solvus crest, carbonate of this composition is on the magnesian calcite side of the solvus, and the assemblage corresponds to calcite-lherzolite. It is of considerable interest to determine the conditions for the existence of dolomite-lherzolite, where the dolomite approaches stoichiometric composition, constrained by the calcite-dolomite solvus.

According to Fig. 7, the invariant point Q is required to generate reaction (6) with stoichiometric dolomite-lherzolite, at lower temperatures than calcite-lherzolite. However, the experimental evidence from Fig. 6 and 7 indicates that reactions (6A) and (9) do not meet at suitable angles to generate the invariant point, Q, and the lower-temperature reaction (6). It can also be shown that reactions (6A) and (9) cannot be in the positions shown by the lines (6A)-a and (9) in Fig. 6; the geometry of the reaction tie-figures makes this impossible.

Another test was made. If we assume that reaction (6A) in Figure 6 is really for dolomite-lherzolite, which requires that the carbonate compositions plotted in Fig. 3 and reported by WYLLIE ET AL. (in press) are in error, and we assume that reaction curves for (6) and (9) intersect with the geometry experimentally determined for (6A) and (9) in Fig. 6, then another array of univariant curves around invariant point Q can be worked out. The result proves to be impossible, because it places reaction (01) on the high-temperature side of reaction (6), which is geometrically incompatible with the tie-figure for reaction (6) (Fig. 1).

Fig. 7 remains the most likely interpretation for the arrangement of reaction curves for stoichiometric dolomite-lherzolite (6) and calcite-lherzolite (6A). If the 10 kb result for reaction (9) had not been reported, the reaction lines for (9) and (6A) could be curved to conform with the theoretical requirement in Figure 7, with the invariant point Q situated somewhere between 7 kbar and 13 kbar. This would be the easiest way to force the experimental curves into a theoretical fit, but probable errors in the results above 15 kbar could also contribute. Given this arrangement, there is need for reconsideration of numbering systems for the reactions. The decarbonation of dolomite-lherzolite is now designated as reaction (6) for two separate reactions. The high-pressure decarbonation reaction for carbonate-lherzolite with solid solution between dolomite and calcite is reaction (6). At temperatures below the calcite-dolomite solvus, this is replaced by two separate reactions, (6A) for magnesian calcite, and (6B) for near-stoichiometric dolomite.

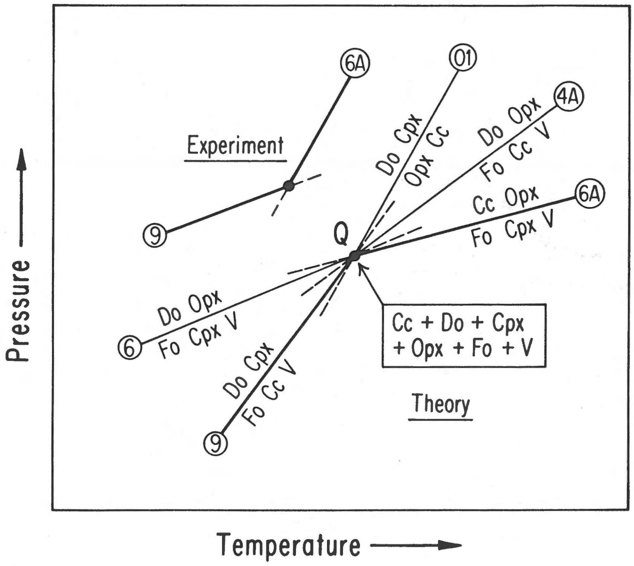

Fig. 7.
The upper left diagram shows the relationship of reactions (6A) and (9) if they intersect in Q, as shown in Fig. 6. The main diagram shows the theoretical array of univariant reactions required by Schreinemaker's rules, given the invariant assemblage occurring at Q (independent determination by E. Woerman, 1983, pers. comm.) Reactions (9) and (6A) in this array do not correspond to the experimental arrangement. The low-temperature reaction (6) for carbonate-lherzolite with carbonate near stoichiometric dolomite should be distinguished as reaction (6B).

The present state of experiment and thermochemistry for establishing the relationships among the reactions (6), (6A), (6B), (9), and (01) is very unsatisfactory. The reactions are close together in terms of PT, the assemblages are resistant to reaction in the laboratory, and the thermodynamic data are inadequate to distinguish among various options which can be deduced from Schreinemaker's rules.

CARBONATION AND MELTING OF MANTLE LHERZOLITE AND HARZBURGITE

Samples of mantle peridotite are transported to the surface in kimberlites and other magmas. Fig. 8 shows the estimated ranges of temperatures and depths of equilibration of some Premier Mine garnet lherzolites and garnet harzburgites, according to DANCHIN (1979). BOYD (1973) correlated such results with fossil geotherms.

Fig. 8 shows phase relationships for model lherzolite and

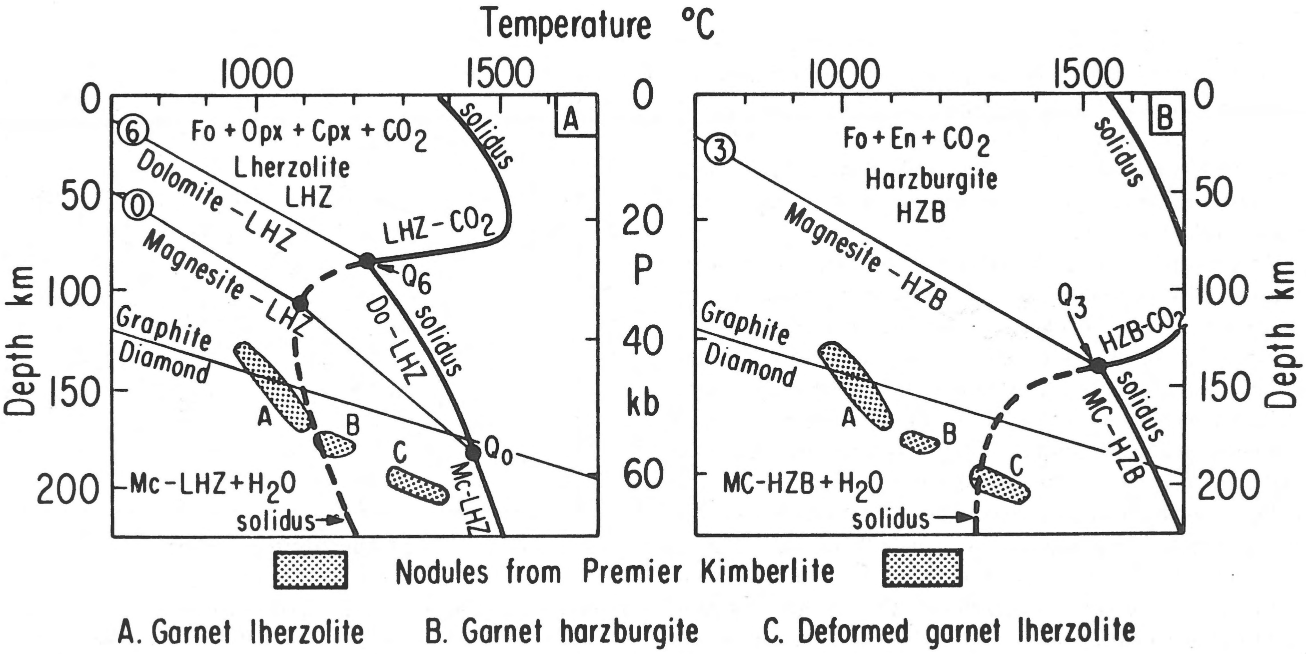

Fig. 8.
Phase diagrams for model lherzolite (LHZ) and harzburgite (HZB) with CO_2, following Wyllie (1977, figure 2) and Wyllie & Huang (1976c, figure 1), with the position of reaction (0) corrected to match BB-p in Fig. 4. Dashed lines are estimated solidus curves with H_2O present as well, after Wyllie (1978, figure 4) and Ellis & Wyllie (1980, figure 9). Areas A, B, and C are estimated depths and pressures of equilibration of some mantle xenoliths from Premier Mine, South Africa (Danchin, 1979).

harzburgite, using the preferred reactions given in Fig. 2, 4, and 5, for subsolidus carbonation and exchange reactions (6), (3), and (0), respectively. These are extended to melting reactions for the model rocks in the presence of moderate amounts of CO_2. Note that the solidus temperatures of the peridotites are not lowered much by CO_2, but there is a large temperature decrease for the solidus curves where the peridotites are carbonated, at pressures above the invariant points Q_6 and Q_3. The dashed lines are estimated solides curves for carbonated peridotites with H_2O added.

These phase diagrams, and the fossil geotherms represented by the shaded areas from Premier Mine peridotites, can be used to make deductions about the petrology of the upper mantle beneath Premier at the time of eruption of the kimberlite, assuming that CO_2 and H_2O were both present, a condition considered to be a prerequisite for the formation of kimberlites (WYLLIE, 1980). At depths greater than about 195 km, both lherzolite and harzburgite would be partially melted. Between about 195 km and 175 km, lherzolite would be partially melted, but magnesite-garnet-harzburgite, if present, would be solid. At depths shallower than 175 km, all peridotites would be solid, with or without CO_2 and H_2O. (Note that these depths are based on phase boundaries for model rock compositions: for real rocks, solidus boundaries would be displaced slightly downwards, and depths would be correspondingly shallower, but the general pattern of results would not change).

Assume that area A consisted of coarse lherzolites and harzburgites uncontaminated by the rising mantle, which is represented by the steep portions of the fossil geotherms, B-C, associated with upward movement of volatile components and kimberlite magma. Eruption of kimberlite from the partially melted lherzolite in regions C and B could be expected to transport to the surface deformed xenoliths of lherzolite, xenoliths of magnesite-harzburgite from area B, and coarse xenoliths from area A. EGGLER (1975) and WYLLIE (1978) suggested that primary carbonates in mantle xenoliths are likely to dissociate rapidly during uprise, after they cross the decarbonation reactions (6) and (3). BOYD & GURNEY (1982) proposed that disseminated magnesite in depleted harzburgites from the base of cratons has caused widespread disruption of garnet-harzburgite nodules. The low-calcium garnets expected in garnet-harzburgites are rare in xenoliths, but common in kimberlites, and probably represent harzburgite xenoliths which exploded through magnesite dissociation during ascent. BOYD & GURNEY (1982) related this to the occurrence of diamonds in the thicker cratons, were deep, depleted harzburgites were carbonated by volatiles from magmatic fluids in the asthenosphere. Fig. 8 demonstrates that solid magnesite-harzburgite could coexist with partly melted lherzolite before eruption, within a specific depth interval.

COMMENT

Professor den Tex and I came together in a Special Issue of 'Tectonophysics' dealing with 'Deep-seated Foundation of Geological Phenomena', based on an Upper Mantle Symposium held at the 23rd International Geological Congress in Prague, 1968. DEN TEX (1969) led the series of discussion papers following my review on 'The origin of ultramafic and ultrabasic rocks' (WYLLIE, 1969). My contribution was an attempt to classify and to distinguish the various kinds of processes which can produce similar ultramafic rocks in various tectonic environments. DEN TEX (1969) presented reasons for subdividing the orogenic peridotites into ophiolitic and 'root-zone' peridotites, and reviewed microstructural, petrofabric approaches to the study of peridotites. From results obtained from root-zone peridotites of Alpe Arami, ophiolitic lherzolite of the French Pyrenees, and lherzolitic nodules from Dreiser Weiher and the Plateau de Velay, he concluded that the most likely origin from all three groups of rocks was 'solid derivation from upper mantle.' DEN TEX (1969) wrote: 'Ophicalcite, a mixture of serpentine and carbonate of mainly dolomitic composition, which is frequently associated with ophiolitic rocks, is often quoted as an arrested stage in the process of serpentinization of carbonate rocks'. Similar rocks can also be produced by the serpentinization and carbonation of peridotites. Conditions for the formation of ophicalcite, with dolomite or calcite, may eventually be deciphered by sorting out the relationships at crustal pressures among reactions (6), (6A), (6B), (9), (01), as discussed above in connection with Fig. 6 and 7.

ACKNOWLEDGEMENTS

This research was supported by the Earth Sciences Section of the National Science Foundation, EAR-8311758. I Thank W.-L. Huang, A. P. Byrnes, and J. Otto for their contributions to this research program, through years at the University of Chicago, and R. C. Newton for consultations, and E. Woermann for discussions.

REFERENCES

Bowen, N. L. 1940 Progressive metamorphism of siliceous limestone and dolomite – J. Geol., 48: 225-274.

Boyd, F. R. 1973 A pyroxene geotherm – Geochim. Cosmochim. Acta, 37: 2533-2546.

Boyd, F. R. & Gurney, J. J. 1982 Low-calcium garnets: keys to craton structure and diamond crystallization – Carnegie Inst. Washington Year Book, 81: 261-267.

Danchin, R. F. 1979 Mineral and bulk chemistry of garnet lherzolite and garnet harzburgite xenoliths from the premier Mine, South Africa. In: F. R. Boyd & H. O. A. Meyer (eds): The Mantle Sample: Inclusions in Kimberlites and Other Volcanics – Am. Geophys. Union, Washington DC: 104-126.

Den Tex, E. 1969 Origin of ultramafic rocks, their tectonic setting and history – Tectonophysics, 7: 457-488.

Eggler, D. H. 1975 Peridotite-carbonate relations in the system CaO-MgO-SiO_2-CO_2 – Carnegie Inst. Washington Year Book, 74: 468-474.

—— 1978. The effect of CO_2 upon partial melting of peridotite in the system Na_2O-CaO-Al_2O_3-MgO-SiO_2-CO_2 to 35 kb, with an analysis of melting in a peridotite-H_2O-CO_2 system – Am. J. Sci., 278: 305-343.

Eggler, D. H., I. Kushiro & J. R. Holloway 1976. Stability of carbonate minerals in a hydrous mantle – Carnegie Inst. Washington Year Book, 75: 631-636.

Ellis, D. & P. J Wyllie 1980. Phase relations and their petrological implications in the system MgO-SiO_2-H_2O-CO_2 at pressures up to 100 kbar – Am. Mineral., 65: 540-556.

Käse, H. R. & P. Metz 1980 Experimental investigation of the metamorphism of siliceous dolomites, IV. Equilibrium data for the reaction: 1diopside + 3dolomite = 2forsterite + 4calcite + $2CO_2$ – Contr. Mineral. Petrol., 73: 151-159.

MacGregor, I. D. 1967 Mineralogy of model mantle compositions. In: P. J. Wyllie (ed.): Ultramafic and related rocks – John Wiley and Sons (New York): 382-393.

Newton, R. C. & W. E. Sharp 1975 Stability of forsterite + CO_2 and its bearing on the role of CO_2 in the mantle – Earth Planet. Sci. Lett., 26: 239-244.

O'Hara, M. J 1967 Mineral facies in ultrabasic rocks. In: P. J. Wyllie (ed.): Ultramafic and related rocks – John Wiley and Sons (New York): 7-18.

Ringwood, A. E. 1966 Mineralogy of the mantle. In: P. M. Hurley (ed.): Advances in Earth Sciences – M.I.T. Press (Cambridge, Mass.): 357-399.

Skippen, G. B. 1971 Experimental data for reactions in siliceous marbles – J. Geol., 79: 457-481.

—— 1974. An experimental model for low pressure metamorphism of siliceous dolomitic marble – Am. J. Sci., 274: 487-509.

Wyllie, P. J. 1969 The origin of ultramafic and ultrabasic rocks – Tectonophysics, 7: 437-455.

—— 1977. Mantle fluid compositions buffered by carbonates in peridotite-CO_2–H_2O – J. Geol., 85: 187-207.

—— 1978. Mantle fluid compositions buffered in peridotite-CO_2–H_2O by carbonates, amphibole, and phlogopite – J. Geol., 86: 687-713.

—— 1980. The origin of kimberlites – J. Geophys. Res., 85: 6902-6910.

Wyllie, P. J. & W.-L. Huang 1975 Peridotite, kimberlite, and carbonatite explained in the system CaO-MgO-SiO_2-CO_2 – Geology, 3: 621-624.

—— 1976a. Petrogenetic grid for siliceous dolomites extended to mantle peridotite compositions and to conditions for magma generation – Am. Mineral., 61: 691-698.

—— 1976b. Carbonation and melting reactions in the system CaO-MgO-SiO_2-CO_2 at mantle pressures with geophysical and petrological applications – Contrib. Mineral. Petrol., 54: 79-107.

—— 1976c. High CO_2 solubilities in mantle magmas – Geology, 4: 21-24.

Wyllie, P. J., W.-L. Huang, J. Otto & A. P. Byrnes in press. Carbonation of peridotites and decarbonation of siliceous dolomites in the system CaO-MgO-SiO_2-CO_2 to 30 kbar – Tectonophysics, 100:359-388.